# Physical Modeling of Clay Slopes in the Drum Centrifuge

JAMES A. CHENEY AND ALI MOHAMAD OSKOOROUCHI

The modeling-of-models technique is used in the physical modeling of overconsolidated kaoline clay embankments by utilizing a drum centrifuge. The clay is consolidated from a slurry in a *g*-field up to 400 times gravity, and then 60° slope embankments from 2 to 8 cm in height are cut and tested for the failure *g*-level. Three types of failure are observed: (a) a quick strength, wherein the *g*-level is raised quickly to failure; (b) a short-term strength, wherein failure takes place in 5-10 min; and (c) long-term failures, which take many hours. The extension of these data to prototype size is tentatively established by tests that vary over a range of scales. This is especially important in establishing a scaling relationship for time. The time-scaling relationship is investigated by observing changes in time to failure as a function of model size for constant prototype dimensions.

The stability of overconsolidated clay slopes was physically modeled by Fragaszy and Cheney (1,2) in a drum centrifuge, shown in Figure 1. Their results indicated that the short-term strength of the slope can be assessed by using the Cam-Clay theory for the yield surface on the dry side of the critical-state line. It was also shown that lower strengths are exhibited in the centrifuge models after a long time (1-12 h) at constant g-level. This experimental finding suggests that it might be possible to model a phenomenon observed in prototype slopes of overconsolidated clay, that of slopes failing after many years of stabile behavior. The results reported (1), however, were not sufficient to establish a scaling relationship between time in the centrifuge and prototype time.

The approach used by Fragaszy and Cheney in centrifuge modeling was to analyze the centrifuge results with a Bishop's-method stability-analysis program by using various choices for the strength parameters. The strength parameters giving factors of safety closest to unity were considered to be closest to correct.

Another approach in centrifuge modeling is to test models over a range of scales to establish the range of validity of the technique and then to make predictions by direct modeling. This approach has been quite successful in applications involving sand (3-5). The application in clay is more complicated because density and water content are self-controlled phenomena in the sense that consolidation depends on internal properties of permeability, compressibility, and viscosity rather than externally controlled deposition. Thus the use of the modeling-of-models technique in clay requires special attention to the initial states of stress and moisture-content distribution in order to satisfy the requirements of similarity between test specimens.

## DRUM CENTRIFUGE

The use of a complete drum for modeling clay slopes has many advantages. It permits the consolidation of clay at extremely high g-levels, and the usual problem of balancing the arm while water is removed in the consolidation process is automatically solved by symmetry. The drum forms its own counterbalance. It permits the study of stability of slopes having no unnatural boundary along their length. However, there are some drawbacks associated particularly with the drum centrifuge that must be addressed.

The drum centrifuge used in this study rotates in a vertical plane and has a very short length (0.3 m) and a radius of 0.6 m. The clay is poured into the drum while the drum is spinning and spreads evenly along the circumference, forming a uniformly thick blanket of clay 0.3 m wide and 0.15 m thick. This blanket is then consolidated under its own weight at 50-400 g by the spinning of the drum. The state of stress during consolidation is in question.

As the layers near the wall of the drum compact, the inner layers must move radially outward. This outward movement must also be accompanied by a circumferential spreading because the layer is moving to a larger radius associated with a larger circumference. The ends of the drum (0.3 m apart) have a camber $\theta$ inward with respect to the plane of rotation so that there must also be an out-of-plane spreading of inner layers as well. The geometry of the drum is shown in Figure 2.

The lateral strains associated with consolidation may be computed from the geometry, the measured inner surface displacement, and the change in water content across the thickness. The radial strain at a given layer is given by the following:

$$\epsilon_v = [\delta v - (d/R^*) - (d/R) + (d^2/RR^*)]/[1 - (d/R^*) - (d/R) + (d^2/RR^*)] \quad (1)$$

in which

$$\delta v = \text{volume change in a layer at depth } d = G_s (w_i - w_f)/(1 + G_s w_i) \quad (2)$$

where

$w_i$ = water content at layer d initially as ratio of dry weight,
$w_f$ = water content at layer d finally,
$G_s$ = specific gravity of clay particles,
$R^*$ = radius of layer from apex of end walls (see Figure 2b),
$R$ = radius of layer from center of revolution of drum (see Figure 2a), and
$d$ = radial displacement of layer.

The displacement d of the surface layer is measured. From this, $\epsilon_v \Delta y$ is subtracted to obtain the displacement d of the second layer. This process has been programmed for high-speed digital computation to determine the displacement distribution and then the lateral strain.

The lateral strain for one test (M-2) is shown in Figure 3. The conditions near the outer wall approach zero lateral strain while conditions near the inner soil surface approach strains large enough to reach the active lateral stress state.

## WATER-CONTENT DISTRIBUTION

The influence of the variable lateral strain on the water-content distribution through the sample can be assessed by use of the Cam-Clay theory (6). If we take

$$\sigma_h' = K \sigma_v' \quad (3)$$

where

$\sigma_v'$ = effective stress in y-direction (radial),
$\sigma_h'$ = effective stress in x, z-directions (lateral), and
$K$ = coefficient of lateral pressure,

Figure 1. Drum centrifuge and peripheral equipment.

Figure 2. (a) Axial view of drum and (b) X-section of drum, A-A.

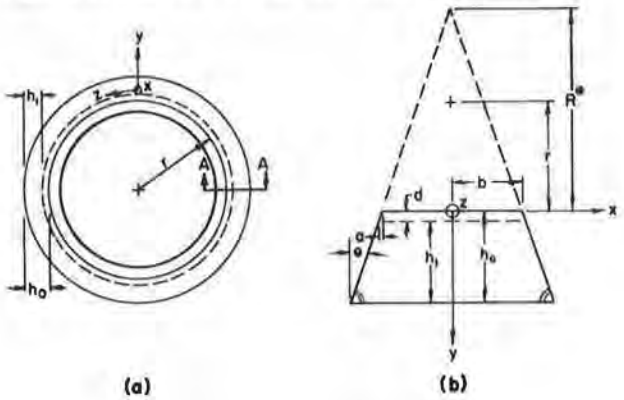


in accordance with the Cam-Clay theory,

$$v = V - \lambda \ell n p' - \{[(\lambda - \kappa)/M]/(q/p')\} \quad (4)$$

where v is the volume of a unit volume of solids,

$$q = \sigma_v' - \sigma_h' = (1 - K)\,\sigma_v' \quad (5)$$

$$p' = (\sigma_v + 2\sigma_h)/3 = [(1 + 2K)/3]/\sigma_v' \quad (6)$$

and V, $\lambda$, $\kappa$, and M are constants of the theory.

The difference in v for $K_o$ conditions (zero lateral strain) and $K_a$ conditions (active Rankine state) is given by the following:

$$\Delta v = v_a - v_o = \lambda \ell n\,[(1 + 2K_o)/(1 + 2K_a)] + [(\lambda - \kappa)/M]\,3\,[(1 - K_o)/(1 + 2K_o)] - [(1 - K_a)/(1 + 2K_a)] \quad (7)$$

Given $\lambda$ = 0.056, $\kappa$ = 0.010, M = 1.27, $K_o$ = 0.5, and $K_a$ = 0.30, the following holds:

$$\Delta v = -0.10 \quad (8)$$

This means that the specific volume for the active Rankine state is less than that for the at-rest state. A smaller specific volume is associated with a smaller water content through the following:

$$\text{water content} = [(v - 1)/G_s] \times 100 \text{ percent} \quad (9)$$

Figure 4 shows schematically the water-content distribution with respect to depth for the $K_a$ (active) and $K_o$ (at-rest) states. The actual

Figure 3. Lateral strain versus depth after consolidation.

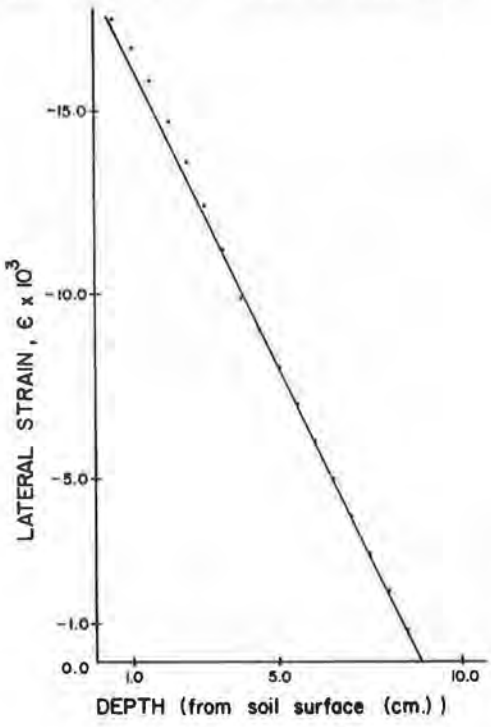


Figure 4. Expected W/C distribution for consolidated soil in drum.

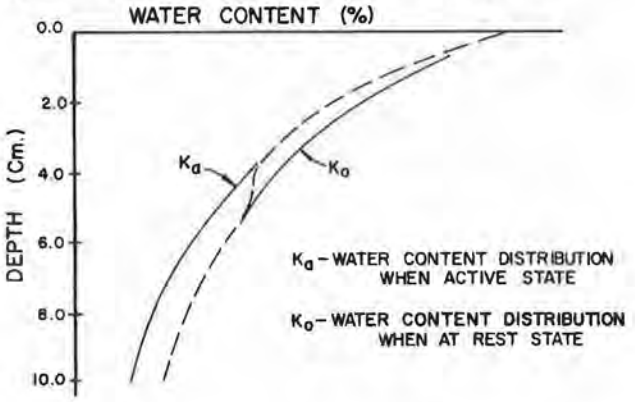


distribution follows the $K_a$-curve in the upper 4 cm of depth and follows the $K_o$-distribution in the lower 4 cm. A transition occurs between these two zones, forming an S shape.

## DESCRIPTION OF TESTS

After consolidation of a clay blanket approximately 9 cm thick, the centrifuge is brought to a stop in order to take moisture-content samples. After this the centrifuge is spun up to the full consolidation speed to return the specimen to the fully consolidated state. Then the centrifuge is slowed to 40-50 rpm and a cutting is made by using a specially shaped cutting tool made of a sharpened wire bent to conform to the shape of the desired slope. The duration of time taken to cut the slope assures that the material is in the fully drained condition after cutting.

The control of the cutting is accomplished by means of a screw-fed rigid bracket to which the

cutting tool is affixed. This mechanism can be seen in Figure 1.

In the quick tests, the centrifuge is then steadily increased in speed, while the circumference is panned with a strobotac triggered by a photo cell that uses a light beam reflected from a target attached to the drum. The speed at which the first sign of a slope failure is observed defines the failure speed and the associated load factor at failure $N_f$.

The quick tests are essentially undrained tests due to the rapid rate of loading, although the analytical results of Fragaszy and Cheney (1) indicate that local dilation may occur at failure. Because the lateral stresses normal to the plane of rotation and the vertical stresses due to self-weight are greatly reduced, the sample is in a highly overconsolidated state. The quick tests are analogous in many respects to a quick draw-down test of a canal embankment.

Timed tests were performed once the quick-test strength had been established. These tests are performed in a similar manner, except the centrifuge speed is set at a percentage of the speed at quick slope failure and the time required to reach failure is observed. Two classes of time behavior are observed: (a) a short-term failure requiring 5-10 min and (b) a long-term failure requiring many hours.

All the slopes tested were at a 60° angle with respect to the horizontal and made of a mixture of kaoline particle sizes (25 percent Mono 90, 75 percent Snow Cal 50) having Cam-Clay properties $\lambda = 0.056$, $\kappa = 0.010$, and $M = 1.27$ and Mohr-Coulomb strength parameters $c' = 0.1$ kg/cm² and $\phi' = 33°$.

## MODELING OF MODELS

It has been stated (3) that the first task of an experimenter is to determine the range of validity of similitude in modeling whenever all the parameters characterizing a prototype are not exactly similar. In the current problem the particle size of the model material is taken as the same throughout the tests at various scales and there is a limit to the size of the model because of the finite length of the drum (0.3 m).

However, it is important also to maintain similarity between model and prototype wherever feasible. Because the strength and deformation characteristics of clay are strongly dependent on the water content, the water-content distribution is an important factor in establishing similarity. The water-content data plotted in Figure 5 were obtained from seven tests, all having the same prototype height but ranging in model height from 2 cm to 8 cm. In order to establish this similarity, it was found necessary to consolidate at the consolidation load factor $N_c$ for 3 h with double drainage, top and bottom.

In order to establish a systematic schedule of quick tests, the array of tests shown in Figure 6 was projected. A prototype height ($H_{pc}$) of 400 cm was chosen for a series of seven model heights, after which tests of six different prototype heights were made at a single model height (5 cm).

The results of these tests are given in Table 1. If scaling is valid, all the tests at the same consolidation prototype height should fail at the same slope prototype height. In Figure 7 the failure prototype heights versus model heights are plotted. The range of consistent results is between 4 and 7 cm.

The divergence of the results for the 8-cm model height appears to be related to the fact that the water content is less than expected for the given consolidation load factor $N_c$. The reason for the divergence at the lower model heights is not clear but may be related to the size of clay conglomerates within the clay mass rather than the size of individual clay particles, and the water-content distribution is significantly different in shape at these lesser model heights.

With the valid range of model height established, a model height midway within this range was chosen for tests of other prototype heights. A plot of these results is given in Figure 8, which shows an almost linear relationship between prototype failure height and prototype consolidation height ($H_{pc}$).

The exception to this trend is test M-25, which, if the line is correct, failed prematurely. This result is explained by the fact that the water-content values for M-25 for some reason were greater than those of M-24, which was consolidated at $N_c$ = 200. Thus, from the water-content data, M-25 should be associated with an $N_c < 175$ and is then in line with the other data points. The water-content plots are given in Figure 9. This observation makes clear that the fundamental parameter in assessing strength of these embankments is the water-content distribution rather than $N_c$. The relation developed between consolidation load factors $N_c$ and failure load factors $N_f$ is simply a convenience for presentation of results.

The relationship of Figure 9 is as follows:

$$H_{p_f} = 140 + 0.24H_{pc} \quad (10)$$

## TIMED TESTS

The initial purpose of the long-duration tests was to establish the length of time necessary (if finite) for a slope lower than its quick-test failure height to fail. Early in the study, it was discovered that there were two types of time-to-failure data, as previously mentioned: a short-term failure requiring 5-10 min to develop and a truly long-term failure requiring many hours.

Table 2 lists the data from the timed tests and these data are plotted in Figure 10 along with the quick-test data for reference. There is a zone of prototype heights in which slopes will fail in a very short period of time. To the right of this zone, the time to failure dramatically increases. Isochrones of failure heights to consolidation heights are developed in the long-term-failure zone.

A cross plot of curves in Figure 10 is shown in Figure 11 that results in a family of time-to-failure lines for constant prototype consolidation height ($N_c \cdot H_m$). These lines are not valid to the left of the dashed line, which represents the boundary between short-term failure and long-term failure.

The test results shown in Figures 10 and 11 are all for a common model height of 5 cm. In order to establish a relationship between the time to failure in the model and time to failure in a prototype, tests over a range of model heights must be performed. To this end, a test series in Table 3 was carried out at a constant prototype height of slope $H_{pF}$ and prototype height in consolidation $H_{pc}$ but with model heights $H_m$ ranging from 4.5 cm to 7.0 cm. The load factors at failure, of course, vary from 98.3 to 63.2.

If the time delay to failure depends on a dispersive phenomenon such as the hydrodynamic delay in consolidation, one would expect the time to be governed by a time factor T, which is proportional to the inverse square of the characteristic length H and directly proportional to time t:

$$T = C_v t/H^2 \quad (11)$$

Figure 5. Water content versus depth in modeling of models.

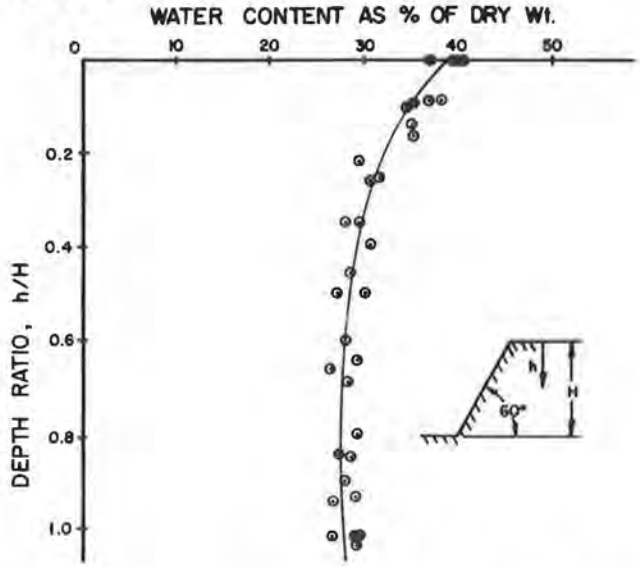


Table 1. Modeling-of-model data.

| Test | $H_m$ (cm) | $N_c$ | $H_{pc}$ (cm) | $N_f$ | $H_{pf}$ (cm) |
|---|---|---|---|---|---|
| M-11 | 2.0 | 200 | 400 | 167 | 334 |
| M-12 | 3.5 | 114 | 400 | 55.2 | 193 |
| M-13 | 4.0 | 100 | 400 | 63.4 | 253 |
| M-14 | 5.0 | 80 | 400 | 47.3 | 236 |
| M-15 | 6.0 | 66.7 | 400 | 39.4 | 236 |
| M-16 | 7.0 | 57.0 | 400 | 34.9 | 244 |
| M-17 | 8.0 | 50.0 | 400 | 37.6 | 301 |
| M-21[a] | 5.0 | 80 | 400 | 47.3 | 236 |
| M-22 | 5.0 | 100 | 500 | 52.4 | 262 |
| M-23 | 5.0 | 150 | 750 | 60.7 | 303 |
| M-24 | 5.0 | 200 | 1000 | 78.0 | 390 |
| M-25 | 5.0 | 250 | 1250 | 70.0 | 350 |
| M-26 | 5.0 | 350 | 1750 | 110.0 | 550 |

[a]Test M-21 is the same as test M-14.

Figure 6. Modeling-of-model test program.

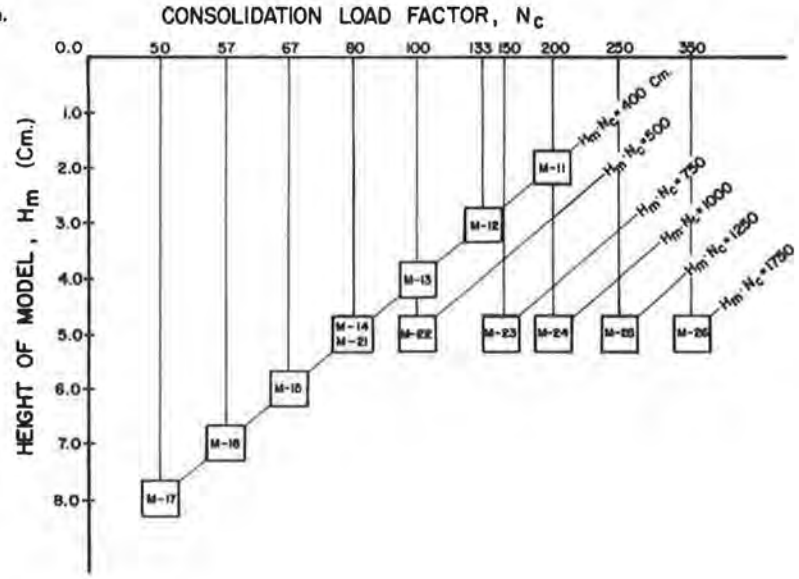


Figure 7. Prototype versus model height for modeling-of-model tests.

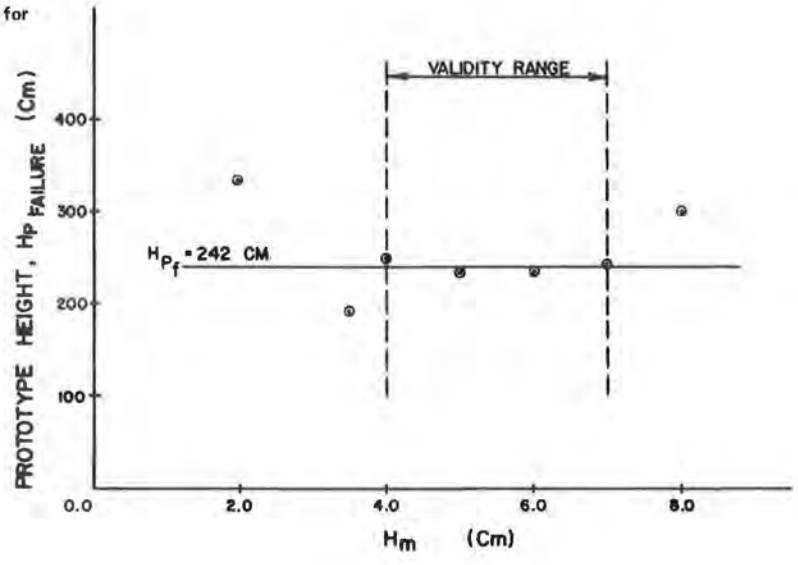

Figure 8. Prototype failure height versus prototype consolidation height for quick tests.

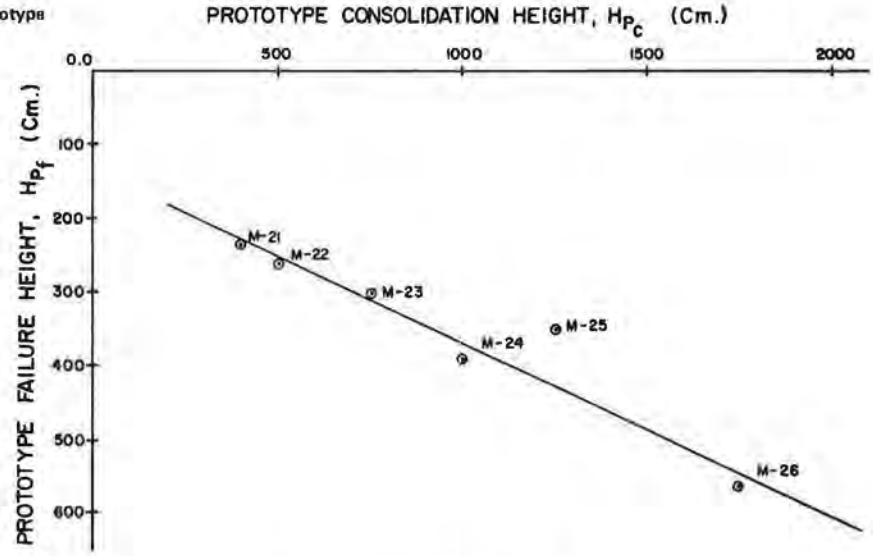


Figure 9. Water-content distribution: quick tests.

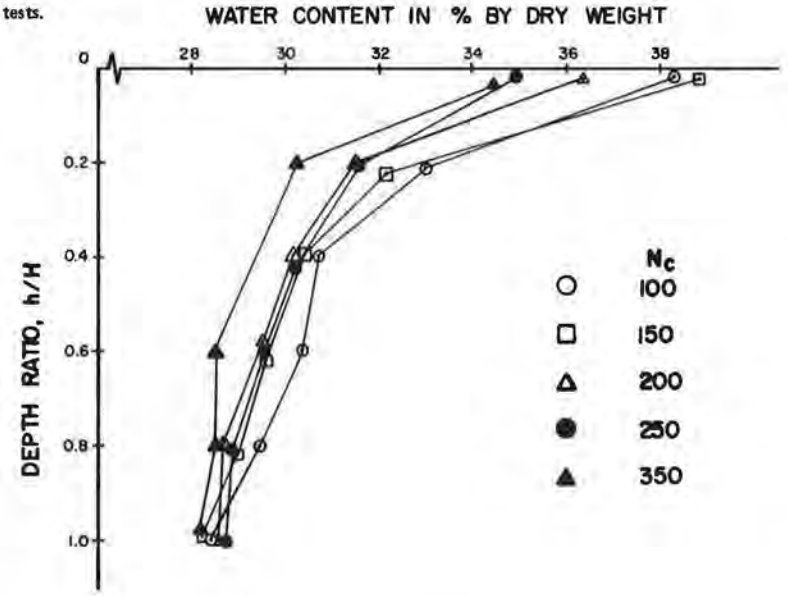


Table 2. Timed-test data.

| Test | $N_c$ | $H_{pc}$ (cm) | $N_f'$ | $H_{pF}$ (cm) | $t_F$ (min) |
|---|---|---|---|---|---|
| M-36 | 350 | 1750 | 88.5 | 442 | 150 |
| M-36A | 350 | 1750 | 77.0 | 385 | 310 |
| M-36B | 350 | 1750 | 54.5 | 272.5 | 520 |
| M-35 | 250 | 1250 | 68.0 | 340 | 295 |
| M-34 | 200 | 1000 | 59.0 | 295 | 5-10 |
| M-34A | 200 | 1000 | 45.0 | 225 | 5-10 |
| M-34B | 200 | 1000 | 39.3 | 196 | 510 |
| M-33 | 150 | 750 | 21.0 | 105 | 5 |

Note: $H_m$ = 5.0 cm.

where $C_v$ is a constant.

The tests in Table 3 were run with constant prototype height; thus,

$$n_f' H_m = 1750 \text{ cm} \quad (12)$$

and

$$n_f'^2 = \overline{1750}^2/H_m^2 \quad (13)$$

The relation between t and $n_f$ becomes the following:

$$t_f = [T(1750)^2/C_v]/(1/n_f'^2) \quad (14)$$

A plot of the inverse square of failure load factor $n_f'$ versus time to failure is given in Figure 12. There is a fair correlation of the data with the theoretical line, and this tends to corroborate Skempton's hypothesis (7) for the time delay to failure. An extrapolation to a load factor of unity gives an estimate of the long-term time to failure of the prototype.

## CONCLUSIONS

The existence of the short-term failure is of great

Figure 10. Results of timed tests.

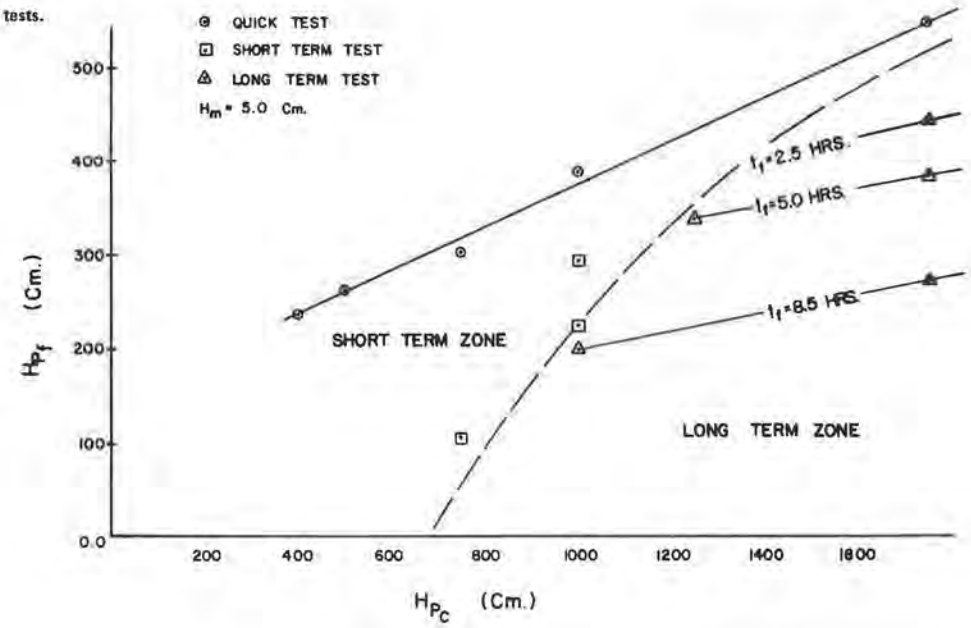


Figure 11. Time to failure (5-cm models).

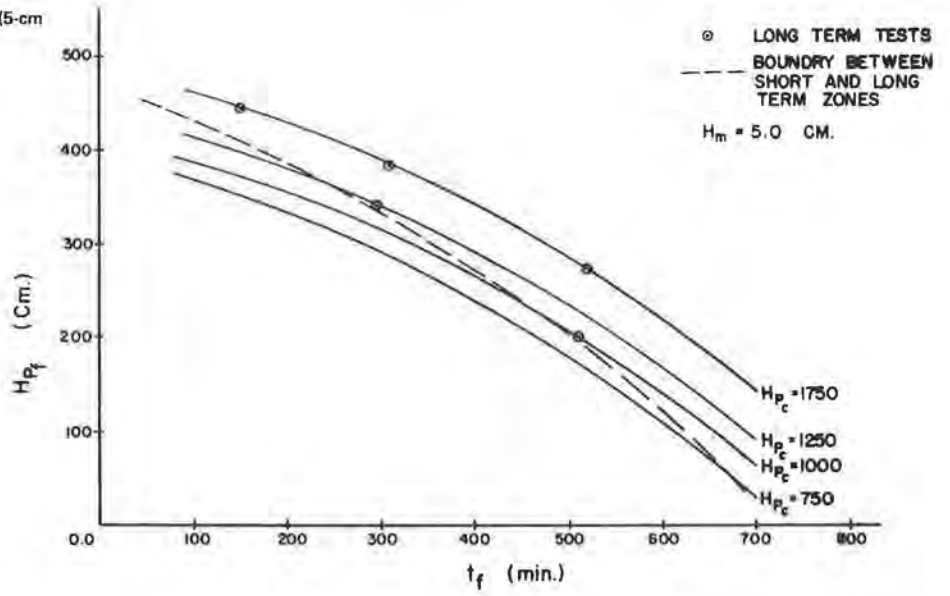


Table 3. Long-term modeling-of-model test data.

| Test | $H_m$ (cm) | $N_c$ | $H_{P_c}$ | $N_f'$ | $H_{P_F}$ | $t_F$ (min) |
|---|---|---|---|---|---|---|
| M-41 | 4.5 | 389 | 1750 | 98.3 | 442 | 10 |
| M-42 | 5.0 | 350 | 1750 | 88.5 | 442 | 150 |
| M-43 | 5.3 | 330 | 1750 | 83.4 | 442 | 88 |
| M-44 | 5.54 | 318 | 1750 | 80.3 | 442 | 72 |
| M-46 | 7.0 | 250 | 1750 | 63.2 | 442 | 180 |

importance in assessment of the safety of slopes. This failure condition is likely associated with a local instability along a failure surface within the clay mass that permits a very localized dilation, leading to a fully softened state (critical state). The existence of this form of failure is suggested by Schofield and Wroth (6) as a mechanism of failure below the yield surface on the dry side of the critical state.

Apparently the quick tests generally were done so fast that such instabilities did not have time to develop, although some scatter in the data might be suggestive of such a reduction in strength.

The long-term behavior clearly exists in the model tests and time to failure increases with the size of the model. This result negates a viscoplastic creep theory (8) as an explanation of the delayed time to failure, which would make modeling invalid. The $N^2$-scaling law used in scaling time for hydrodynamic events (seepage, consolidation) appears to govern generally the delay time to failure and therefore corroborates the theory of Skempton (7).

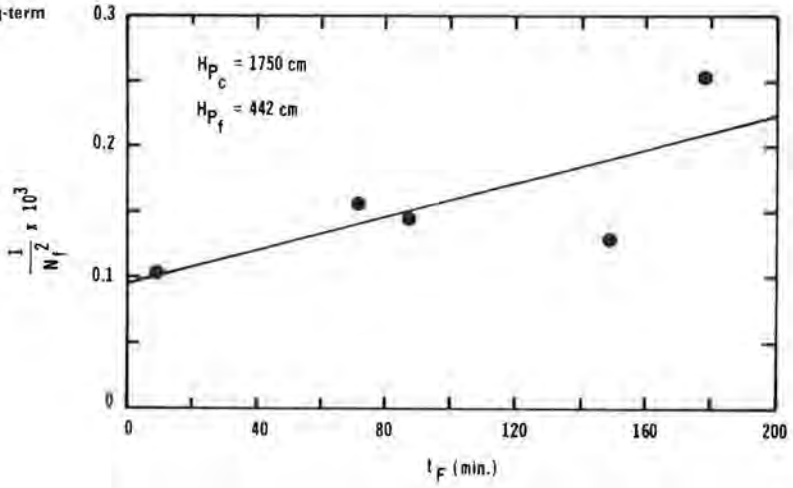


Figure 12. Time to failure versus $1/N_f^2$ for long-term modeling-of-model test.

REFERENCES

1. R. Fragaszy and J.A. Cheney. Drum Centrifuge Studies of Overconsolidated Slopes. Journal of Geotechnical Engineering Division of ASCE, Vol. 107, No. GT7, 1981, pp. 843-858.
2. R. Fragaszy. Drum Centrifuge Studies of Overconsolidated Clay Slopes. Univ. of California, Davis, Ph.D. dissertation, 1979.
3. N. Krebs-Ovesen. Centrifuge Testing Applied to Bearing Capacity Problems of Footings on Sand. Geotechnique, Vol. 25, 1975, pp. 344-401.
4. N. Krebs-Oveson. The Scaling Law Relationships. Proc., Seventh European Conference on Soil Mechanics and Foundation Engineering, Brighton, England, 1979, Vol. 4, pp. 319-323.
5. N. Krebs-Oveson. Centrifuge Tests to Determine the Uplift Capacity of Anchor Slabs in Sand. Proc., 10th International Conference on Soil Mechanics and Foundation Engineering, Stockholm, Sweden, 1981.
6. A.N. Schofield and C.P. Wroth. Critical State Soil Mechanics. McGraw-Hill, London, 1968.
7. A.W. Skempton. Slope Stability of Cuttings in Brown London Clay. Proc., Ninth International Conference on Soil Mechanics and Foundation Engineering, Tokyo, Vol. 3, Special Lectures, 1977, pp. 261-270.
8. J.D. Nelson and E.G. Thompson. A Theory of Creep Failure in Overconsolidated Clay. Journal of the Geotechnical Engineering Division of ASCE, Vol. 103, No. GT11, 1977, pp. 1281-1294.

*Publication of this paper sponsored by Committee on Mechanics of Earth Masses and Layered Systems.*

# Centrifugal Testing of Soil Slope Models

MYOUNG MO KIM AND HON-YIM KO

**The principles of testing static geomechanical models are explained, and the need to simulate the gravity-induced body forces is emphasized. The only convenient method of inducing increased gravity on models of soil structures is to spin the model in a centrifuge. Experiments were conducted in a 10-*g*-ton geotechnical centrifuge to model the stability of slopes of partly saturated granular soils. A series of modeling-of-models tests was conducted in which several models of different scales were tested at different gravity scales. The internal consistency of the centrifugal modeling technique is demonstrated by results of these tests, which show that the same critical height of the prototype slope is obtained irrespective of model scale. A quantitative comparison is made of the model test data and analytical results from limit analysis, finite-element analysis, and limiting-equilibrium analysis. It is demonstrated that the critical slope heights obtained from the centrifuge tests are bracketed within the upper bounds established by limit analysis and the lower bounds obtained from finite-element calculations. In addition, the locations of the failure surface obtained by testing and analysis correspond closely in all cases.**

Testing of scaled earth models under an increased gravitational body force field is a relatively new idea in soil mechanics. This centrifugal-modeling technique is the only method that can completely satisfy the requirements of the principles of similitude in the geotechnical model in which body forces of a structure are significant. Nevertheless, many workers are still unconvinced of the validity of the method, primarily due to the lack of prototype data against which model behavior can be compared. Even when such data are available, comparisons usually point out the necessity to better define the geology of the prototype situation as well as the material properties.

In order to demonstrate that the scaled centrifugal model can project to prototype behavior, it is possible to carry out a modeling of models, in which a series of models is constructed at different scales, all representing the same prototype (which could be an imaginary situation), and tested at different gravity ratios, each calculated to bring the respective model to full similitude with the prototype. Only when it has been demonstrated that